Internally Compensated, Externally Pressurized Gas Bearings

By A. L. Carpenter, B.E.(Hons.), Stud.I.E.Aust. and J. Mannam, Ph.D., M.I.E.Aust.*

Summary.—This paper discusses the theoretical and experimental investigation of internally compensated gas bearings of the tapered land type. The results of the theoretical analysis, which are closely confirmed by experimental evidence lead to the conclusions that:

(1) The Reynolds equation for compressible flow can be used to evaluate the pressure distribution in the clearance space (and hence the load capacity and the leakage flow) for the range of operating conditions considered.
(2) The effect of lubricant compressibility is to decrease the load-carrying capacity and to increase the leakage flow.
(3) For the range of tests considered, isothermal conditions may be assumed.
(4) For length/diameter ratios in the range 0 to 2 the optimum taper/clearance ratio is in the region of 1.
(5) At any given pressure ratio the load coefficient varies approximately linearly with eccentricity ratio.
(6) The effect of length/diameter ratio on the leakage flow is negligible.
(7) Adequate information can be presented to enable bearings of the tapered land type to be designed for any practical application.

LIST OF SYMBOLS

Variables:

c Radial clearance at large end of land.
d Nominal bearing diameter.
e Eccentricity.
f Elemental force or load.
F Total force or load on one land.
h Clearance at position (x, y).
l Land length $= \frac{1}{2}$ (bearing length).
m Elemental righting moment.
M Total righting moment on one land.
p Pressure at position (x, y).
p_1 Supply pressure.
p_2 Discharge pressure.
Δp Pressure drop through bearing $= (p_1 - p_2)$.
q Elemental leakage flow.
Q Total leakage flow past one land.
r Nominal bearing radius.
t Radial taper decrement over length of land.
u x-component of fluid velocity.
x Axial location co-ordinate.
y Circumferential location co-ordinate.
z Radial location co-ordinate.
δ Displacement.
μ Dynamic viscosity of lubricant fluid.
ρ Density of lubricant fluid.
θ Angular position, measured from point of minimum clearance.

Subscripts:

f Force or load.
m Moment.
q Flow.
t Tilted.
x, y Location in xy plane.

Dimensionless Ratios and Coefficients:

A Angularity ratio $= \dfrac{e_t}{c}$.

C_f Load coefficient $= \dfrac{F}{\Delta p \,.\, l \,.\, d}$.

C_q Flow coefficient $= \dfrac{Q \,.\, \mu \,.\, l}{\Delta p \,.\, d \,.\, c}$.

C_m Moment coefficient $= \dfrac{M}{\Delta p \,.\, l^2 \,.\, d}$.

E Eccentricity ratio $= \dfrac{e}{c}$.

H Dimensionless clearance $= \dfrac{h}{c}$.

K Constant in the isothermal equation.

L Length ratio $= \dfrac{l}{r} = \dfrac{2 \,.\, l}{d}$.

P Dimensionless pressure $= \dfrac{p}{\Delta p}$.

PR Pressure ratio $= \dfrac{p_1}{p_2}$.

T Taper ratio $= \dfrac{t}{c}$.

X Dimensionless axial location parameter $= \dfrac{x}{l}$.

Y Dimensionless circumferential location parameter $= \dfrac{y}{2\pi r}$.

INTRODUCTION

It is a now well-known fact that in the field of gas-film lubrication externally pressurised bearings are the type most commonly used. The reasons for this are that they can support greater loads than can self-acting bearings, they avoid the wear undergone by self-acting bearings during starting and stopping and they exhibit stability characteristics that are superior to those of the self-acting type.

Hitherto various workers in this field reported on investigations carried out on externally pressurised bearings of a design now referred to as the externally compensated type. These bearing assemblies (Fig. 1) consisted essentially of a cylindrical journal and a bearing shell having a set of orifices drilled into it. The orifices had to be carefully matched to the clearance and difficulties were encountered in drilling the small sizes of holes necessary to obtain the required load characteristics. Extremely accurate positioning of these holes was also found to be necessary to avoid instabilities.

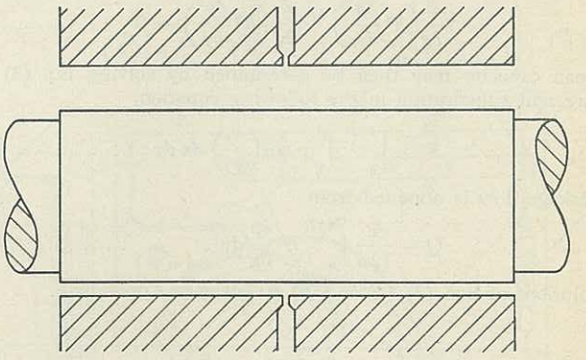

Fig. 1.—*Externally Compensated Journal Bearing.*

An investigation was initiated at the University of Adelaide to examine the characteristics of a different type of externally pressurised bearing, referred to in this paper as *the internally compensated bearing*. In this case the journal has a central annulus (Fig. 2) and the flow through the clearance is restricted by a taper on the lands. The degree of the restriction will depend on the position of the journal within the shell.

This paper discusses the results obtained from the theoretical and experimental investigation of internally compensated gas bearings of the tapered land type. The effect of taper/clearance ratio, length/diameter ratio and eccentricity on the load carrying capacity and leakage flow are presented.

*Paper No. 2582 presented at the Third Australasian Conference on Hydraulics and Fluid Mechanics held in Sydney from 25th to 29th November, 1968.

Mr. Carpenter is a Post-graduate Research Student and Dr. Mannam is Reader, Department of Mechanical Engineering, University of Adelaide.

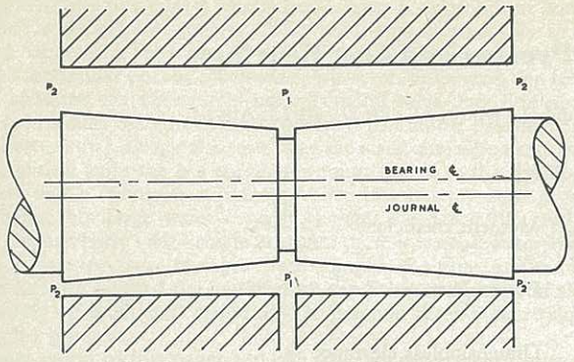

Fig. 2.—Internally Compensated (Tapered Land) Journal Bearing.

THEORETICAL CONSIDERATIONS

Fig. 2 shows the configuration of an internally compensated bearing. The assembly consists of a cylindrical shell and a journal of dumb-bell form, tapered to produce a converging clearance in the direction of flow. High pressure air is fed to the central annulus at P_1 and is allowed to leak through to clearance to a pressure P_2. If the journal is concentric with the bearing the pressure in any plane perpendicular to the axis will be constant around the clearance and no out of balance force will exist. However if the journal is displaced radially in the bearing then the pressure in a plane perpendicular to the axis will no longer be equally distributed around the clearance, and an out of balance force will be created tending to centralise the journal. For a given delivery pressure P_1, the magnitude of this force will depend on the position of the journal and will be a maximum when it contacts the bore.

It should perhaps be mentioned that the same effect will be produced if the tapers were provided in the bearing and the journal was made cylindrical. However, practical considerations would favour the former arrangement.

The governing equation for the pressure distribution in the clearance space is given by

$$\frac{\partial}{\partial x}\left(\frac{\rho h^3}{\mu}\cdot\frac{\partial p}{\partial x}\right)+\frac{\partial}{\partial y}\left(\frac{\rho h^3}{\mu}\cdot\frac{\partial p}{\partial y}\right)=0 \quad \text{.....(1)}$$

Previous investigators (Ref. 1) have already established that the flow in the clearance may be assumed to be isothermal. Therefore, over a wide range of operating conditions the viscosity can be taken to be constant. Furthermore, the isothermal equation

$$\frac{p}{\rho}=K \quad \text{.....(2)}$$

may be used, and combining this with Eq. (1) yields:—

$$\frac{\partial}{\partial x}\left(h^3\frac{\delta p^2}{\partial x}\right)+\frac{\partial}{\partial y}\left(h^3\frac{\partial p^2}{\partial y}\right)=0 \quad \text{.....(3)}$$

The load capacity may then be determined by solving Eq. (3) for the pressure and substituting in the following equation,

$$F=\int_0^{2\pi R}\int_0^{l} p\cos\left(\frac{y}{r}\right)dx\,dy \quad \text{.....(4)}$$

The leakage flow is obtained from

$$Q=\frac{1}{12\mu}\int_0^{2\pi R} h^3\frac{\partial p}{\partial x}dy\Big|_{x=0 \text{ or } l} \quad \text{.....(5)}$$

The solutions of Eqs. (3), (4) and (5) are given in Appendix I.

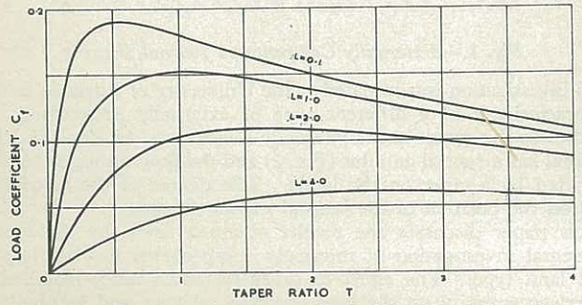

Fig. 3.—Load Coefficient against Taper Ratio (for $L = 0.1$ to 4.0, $E = 1.0$, $PR = 4.4$).

Load Carrying Capacity :

The relationship between the load coefficient and the taper ratio for several values of the length ratio is shown in Fig. 3, where the load carrying capacity of the bearing is represented by a non-dimensional load coefficient, given by

$$C_f=\frac{F}{\Delta p\,.\,l\,.\,d} \quad \text{.....(6)}$$

It will be noticed that for any given length ratio the load coefficient reaches a maximum at a particular value of the taper ratio. For length ratios in the range 0 to 2 this value is in the region of 1, and increases as the length ratio is increased. It will also be seen that, for a given taper ratio, the load coefficient decreases as the length ratio increases. This may be explained as follows.

The friction path of the fluid in long bearings will be greater in the axial than in the circumferential direction. For this reason short circuiting (circumferential) flow will take place which will have the effect of reducing the load carrying capacity. This phenomenon is at the present under investigation.

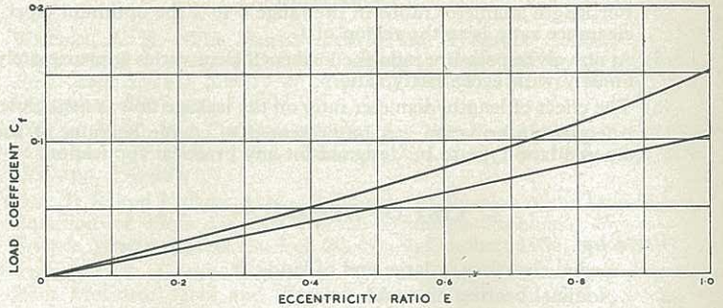

Fig. 4.—Load Coefficient against Eccentricity Ratio (for $L = 2.0$ and 1.0, $T = 1.0$, and $PR = 4.4$).

Fig. 4 illustrates the way the load coefficient varies with eccentricity for the two cases $L = 1$ and $L = 2$. The general trend of these curves indicates that the stiffness of this type of bearing increases with increasing eccentricity. This result is at variance with the stiffness characteristic of the externally compensated type of bearing where stiffness falls off considerably with eccentricity ratios above 0.6.

Leakage Flow :

Fig. 5 shows the effect of the taper ratio on the leakage flow for several values of the length ratio. The leakage flow is represented by a non-dimensional flow coefficient given by

$$C_q=\frac{q\,\mu\,l}{\Delta p\,.\,d\,.\,c^3}$$

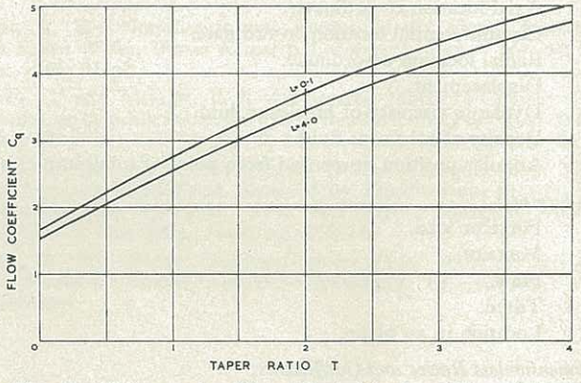

Fig. 5.—Flow Coefficient against Taper Ratio (for $L = 0.1$ and 4.0, $E = 1.0$, $PR = 4.4$).

It will be observed that the effect of length ratio on the flow coefficient is negligible. However the flow coefficient increases substantially with taper ratio. Fig. 6 shows the effect of eccentricity ratio on the flow coefficient.

The Effect of Pressure Ratio :

It should be pointed out that the curves presented in Figs. 3 to 6 were computed for an inlet pressure of 50 lb. /sq. in. g., and an outlet pressure of zero lb. /sq. in. g. In previous work (Ref. 2) with incompressible fluids the non-dimensional load coefficient C_f and flow coefficient C_q were found

to be independent of the pressures at the inlet and outlet boundaries of the bearing. However, for a gas lubricated bearing this condition no longer holds.

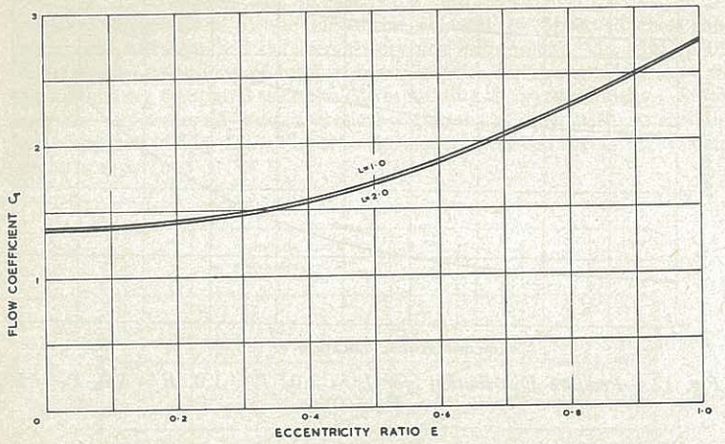

Fig. 6.—*Flow Coefficient against Eccentricity Ratio* (*for* $L = 1.0$ *and* 2.0, $T = 1.0$, $PR = 4.4$).

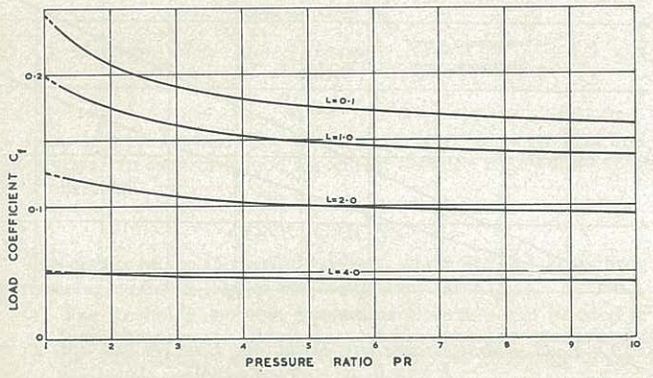

Fig. 7.—*Load Coefficient against Pressure Ratio* (*for* $L = 0.1$ *to* 4.0, $T = 1.0$, $E = 1.0$).

The effect of pressure on the load coefficient can be seen in Fig. 7. It will be noticed that at high pressure ratios the load coefficient is virtually constant, but increases sharply at low pressure ratios. The curves of Fig. 7 may be extrapolated to the ordinate for a pressure ratio of 1. The intercepts will yield values of the load coefficient C_f which are in close agreement with those obtained for incompressible flow (Ref. 2). This is to be expected, since at very low pressure ratios the behaviour of the gas approaches that of an incompressible fluid.

Angular Stiffness :

In many practical applications a gas lubricated journal bearing may not only be required to support a radial load, but also to keep angular misalignment of the journal and bearing axes within certain design limits. A knowledge of the bearing's ability to resist these angular deflections (called here the angular stiffness) is therefore of considerable importance. For this reason it was decided to examine the effect of the taper ratio and length ratio on the angular stiffness of the tapered land bearing.

For a given journal/bearing configuration the value of the angular stiffness will depend on the angle between the journal and the bearing axes. This will be a maximum when the two lands of the journal contact the bearing shell as shown in Fig. 8. This position was therefore chosen for the analysis.

An expression for h describing the local clearance under the tilted condition was first derived as shown in Appendix II and then Eq. (3) was solved for pressure as before. The righting moment was then determined from

$$M = \int_0^{2\pi R} \int_0^{l} \rho \cos\left(\frac{y}{r}\right) . (l - x) . dx . dy \qquad \text{.....(7)}$$

The solution of Eq. (7) is given in Appendix II.

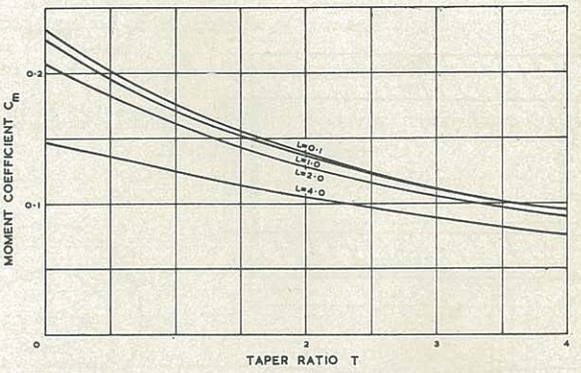

Fig. 9.—*Moment Coefficient against Taper Ratio* (*for* $L = 0.1$ *to* 4.0, $PR = 4.4$, $E = 1.0$).

The relationship between the righting moment and the taper ratio for various length ratios is shown in Fig. 9, with the righting moment presented in the form of a non-dimensional moment coefficient, C_m, where,

$$C_m = \frac{M}{\Delta P . l^2 . d} \qquad \text{.....(8)}$$

It will be noticed that the max. moment coefficient for a given length ratio occurs at the Taper Ratio = 0—i.e., for a parallel land journal.

EXPERIMENTAL APPARATUS AND TEST PROCEDURE

The apparatus (Fig. 10) consisted essentially of the bearing (1) which contained the journal (2) rigidly fixed to the base plate (3). The bearing was held in a cradle (4) which was suspended from one end of a counterbalanced lever (5). A spring balance (6) attached to the other end of the lever measured the load which was applied by means of a geared capstan (7).

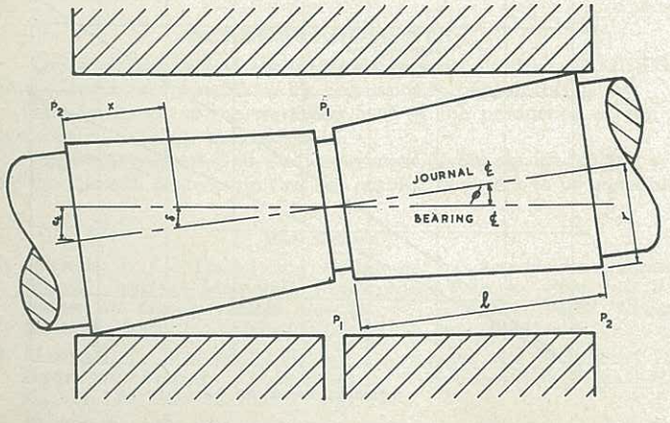

Fig. 8.—*Fully Tilted Tapered Land Journal Bearing.*

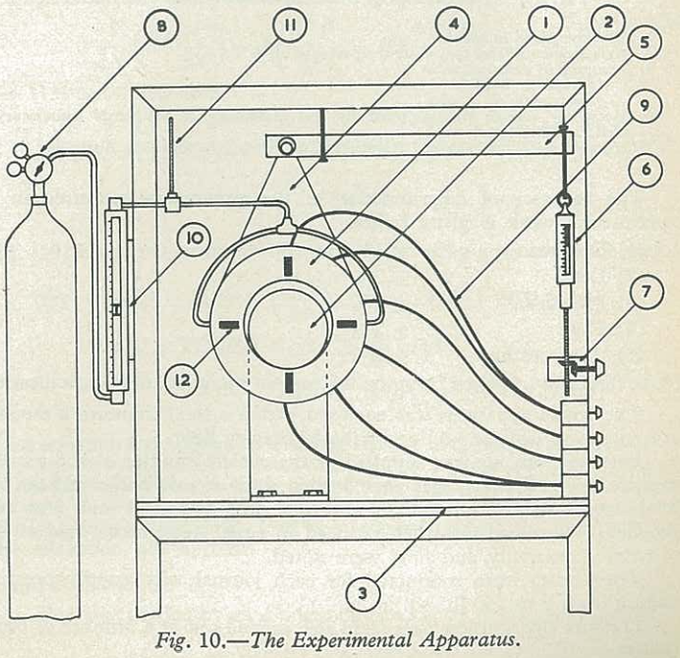

Fig. 10.—*The Experimental Apparatus.*

Air under pressure was supplied to the central annulus from an air bottle (8). A set of pressure tappings (9) arranged around the bearing surface enabled the pressure distribution in the clearance to be determined. The leakage through the clearance was measured with a flowrator (10), and thermometers (11) were used to measure the air temperature at inlet and outlet. Induction type displacement transducers (12) positioned at each end of the bearing assembly gave a continuous and accurate indication of the relative position of the bearing and journal during the tests.

The bearing and journals were made from dimensionally stable oil hardening steel, and the surfaces were finished ground. Fig. 11 shows the salient dimensions of the test pieces. The variations of the bearing and journal from true circularity (given in Fig. 11) are significant only in a small region near the contact point. The pressure distribution in the clearance space in this region could be slightly affected, but it was considered that the overall effect of these dimensional variations on the load and flow characteristics would be negligible.

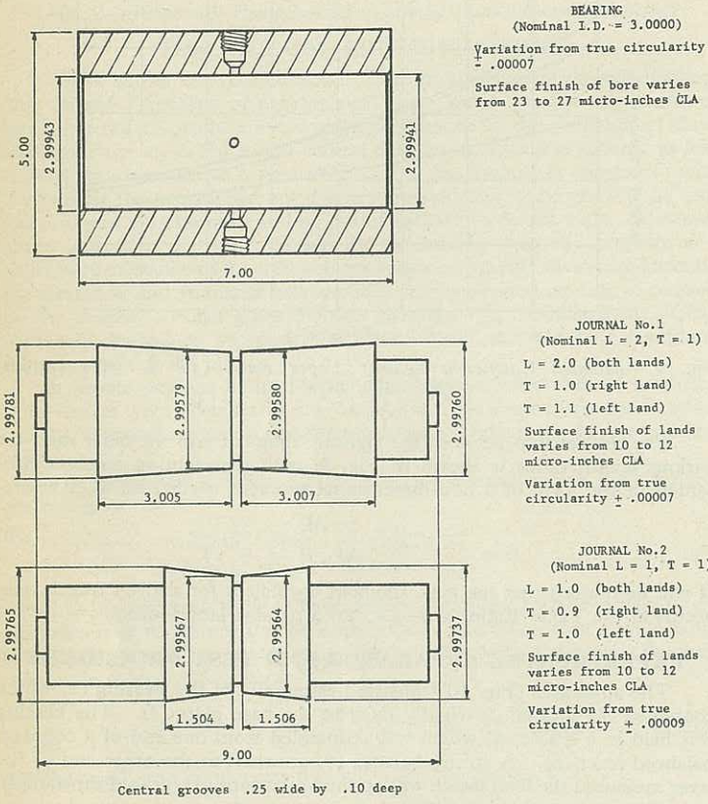

Fig. 11.—*Dimensions of the Test Bearing and Journals.*

NOTES:
1. All dimensions in inches.
2. Measurements refer to a basic temperature of 68°F.
3. Accuracy of determination
   Linear ± .000 04
   Surface finish ± 10%.
4. Metrology service was supplied by the Metrology & Standards Laboratory of W.R.E., Salisbury.*

*Registered with the National Association of Testing Authorities, Australia.

The accuracy of determination of the parameters measured in the experimental work is given below.

(1) Eccentricity	± 1%
(2) Load	± 2%
(3) Pressure	± 2%
(4) Flow	± 2%
(5) Temperature	± 2%

These figures were taken from the instrument manufacturers' specifications.

The whole apparatus was enclosed within a rigid framework mounted on a vibration isolated section of the laboratory floor.

For the tests, air was supplied to the central annulus at the required pressure. The bearing was then loaded until it just made contact with the journal—the fully eccentric position—and the load and flow were recorded. The load was then reduced in equal decrements, and at each load the eccentricity and flow were noted.

These tests were conducted for each journal with supply pressures ranging from 5 to 150 lb. /sq. in. g.

Pressure distribution tests were also carried out at a number of eccentricities.

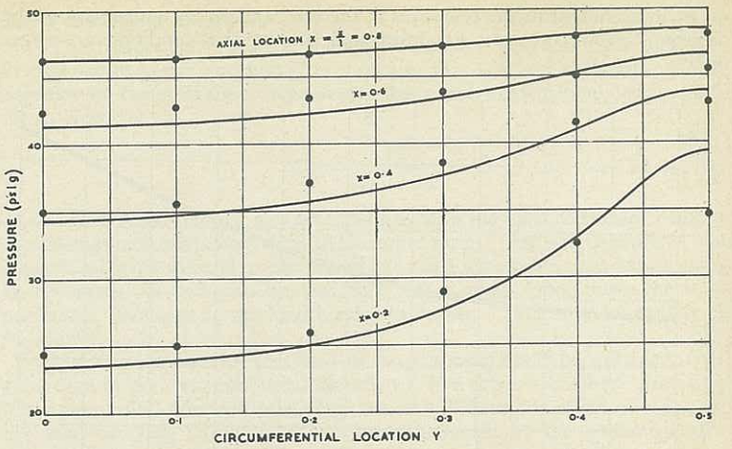

Fig. 12.—*Pressure Distribution (for* $L = 2.0$, $T = 1.0$, $E = 1.0$, $P_1 = 50$, $P_2 = 0$).

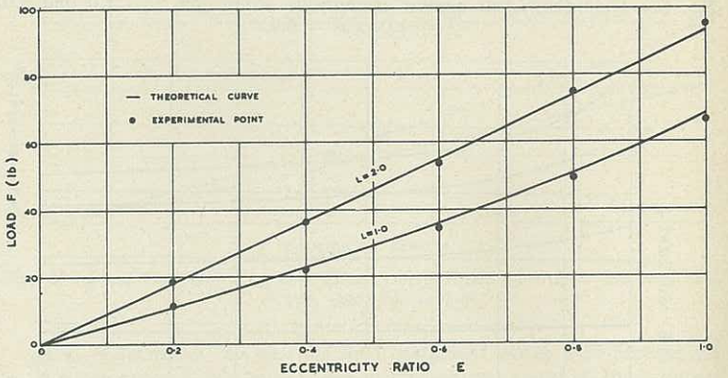

Fig. 13.—*Load against Eccentricity Ratio (for* $L = 1.0$ *and* 2.0, $T = 1.0$, $E = 1.0$, $P_1 = 50$, $P_2 = 0$).

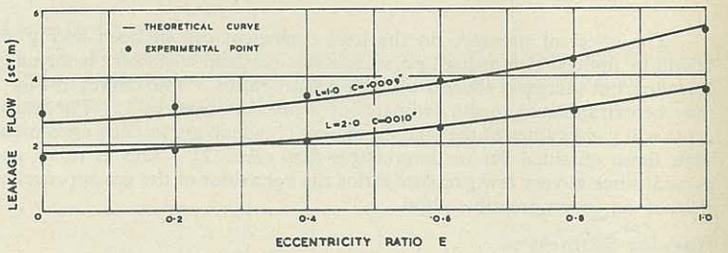

Fig. 14.—*Leakage Flow against Eccentricity Ratio (for* $L = 1.0$ *and* 2.0, $T = 1.0$, $E = 1.0$, $P_1 = 50$, $P_2 = 0$).

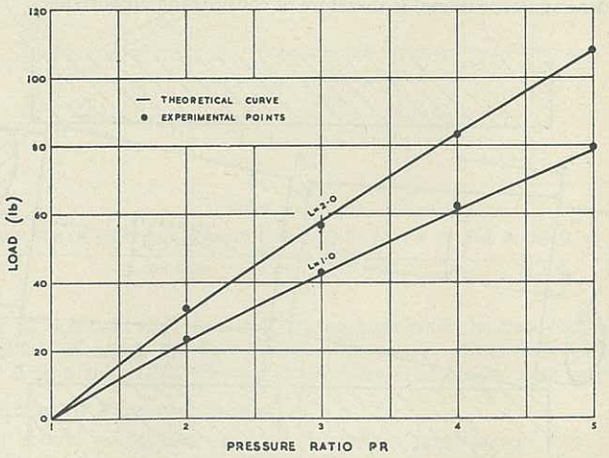

Fig. 15.—*Load against Pressure Ratio (for* $L = 1.0$ *and* 2.0, $T = 1.0$, *and* $E = 1.0$).

TEST RESULTS

The experimental tests were designed to establish the validity of the theoretical findings.

Fig. 12 compares the experimental and theoretical results of the pressure distribution in the clearance. It will be observed that good agreement was obtained between theory and experiment. In Fig. 13 the experimental variations of load with eccentricity for the two bearing configurations are compared with the corresponding theoretical values. Similarly the experimental and theoretical variations of flow with eccentricity are compared in Fig. 14. The close agreement between theory and experiment is apparent.

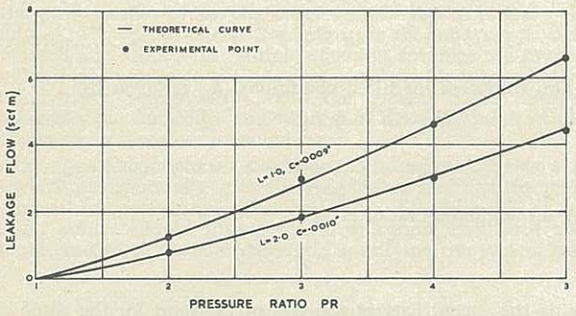

Fig. 16.—*Leakage Flow against Pressure Ratio (for* $L = 1.0$ *and* 2.0, $T = 1.0$, $E = 1.0$).

Figs. 15 and 16 show the effect of pressure ratio on load and flow respectively. In each case good agreement between theory and experiment will be observed.

CONCLUSIONS

The results of the theoretical analysis, which are closely confirmed by experimental evidence, lead to the conclusions that:

(1) The Reynolds equation for compressible flow can be used to evaluate the pressure distribution in the clearance space (and hence the load capacity and the leakage flow) for the range of operating conditions considered in this paper.

(2) The effect of lubricant compressibility is to decrease the load carrying capacity and to increase the leakage flow.

(3) For the range of tests considered, isothermal conditions may be assumed.

(4) For length ratios in the range 0 to 2 the optimum taper ratio is in the region of 1.

(5) At any given pressure ratio the load coefficient varies approximately linearly with eccentricity ratio.

(6) The effect of length ratio on the flow coefficient is negligible.

(7) Adequate information can be presented to enable bearings of the tapered land type to be designed for any practical application.

FURTHER WORK

(1) It is proposed to examine the pneumodynamic characteristics of the tapered land journal bearing.

(2) Modifications to the bearing configuration to improve unidirectional load carrying capability will be investigated.

(3) The effect of high pressure ratios on the load carrying capacity and leakage flow will also be examined.

ACKNOWLEDGMENTS

The work was carried out under the aegis of Professor H. H. Davis, and the authors are grateful for his permission to publish this paper.

The assistance of the workshop staff in the production of the test apparatus is gratefully acknowledged.

Thanks are also due to the Department of Supply for making available the research studentship that has enabled this work to be undertaken.

References

1. Ausman, J. S.—Theory and Design of Self-Acting Gas-Lubricated Journal Bearings Including Misalignment Effects. *First Int. Symposium on Gas-Lubricated Bearings. U.S. Office Naval Research, Research Report No.* ACR-49, Oct., 1959, pp. 161-92.
2. Mannam, J., Fowler, J. H. and Carpenter, A. L.—Tapered Land Hydrostatic Bearings. *Lubrication and Wear Convention, Proc. I. Mech. E.*, Vol. 179, 1964-65, *Part* 3*J*, pp. 78-84.
3. Southwell, Sir Richard Vynne—*Relaxation Methods in Theoretical Physics*, Vol. 1. Oxford, Clarendon Press, 1946, 2 vols., 522 p.
4. National Physical Laboratory—*Notes on Applied Science No.* 16, 1961. Modern Computing Methods. 2nd ed. rev. London, H.M. S.O., 1961.
5. Hildebrand, F. B.—*Introduction to Numerical Analysis.* New York, McGraw-Hill, 1956, 511 p.

APPENDIX I

Calculation of Film Thickness :

From Fig. 17:

$$(O'A)^2 + (AB)^2 = (O'B)^2 \quad \text{.....(9)}$$

therefore

$$(r\cos\theta - e)^2 + (\sin\theta)^2\left(r - \frac{x}{l}t - c + h\right)^2 \quad \text{.....(10)}$$

Neglecting second-order terms in c, e, h and θ yields:

$$h = c + \frac{x}{l}t - e\cos\theta \quad \text{.....(11)}$$

Dividing Eq. (11) by c gives the film thickness in non-dimensional form:

$$H = 1 + XT - E\cos(2\pi Y) \quad \text{.....(12)}$$

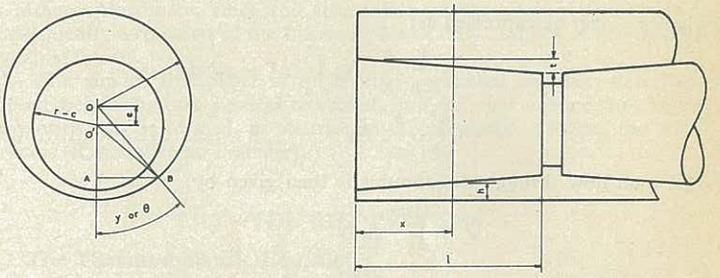

Fig. 17.—*Diagrammatic Representation of the Journal and Bearing.*

Difference Solution of Reynolds Equation :

The form of Reynolds Equation to be solved was given in Eq. (3), i.e.,

$$\frac{\partial}{\partial x}\left(h^2\frac{\partial p^2}{\partial x}\right) + \frac{\partial}{\partial y}\left(h^2\frac{\partial p^2}{\partial y}\right) = 0$$

To obtain a generalized solution, Eq. (3) can be converted into non-dimensional form, giving

$$\frac{\partial}{\partial X}\left(H^3\frac{\partial P^2}{\partial X}\right) + \left(\frac{L}{2\pi}\right)^2 \cdot \frac{\partial}{\partial Y}\left(H^3\frac{\partial P^2}{\partial Y}\right) = 0 \quad \text{.....(13)}$$

Using an identity given by Southwell (Ref. 3), namely

$$2\frac{\partial}{\partial X}\left(H^3\frac{\partial P^2}{\partial X}\right) = \partial^2\frac{H^3P^2}{\partial X^2} + H^3\frac{\partial^2(P^2)}{\partial X^2} - P^2\frac{\partial^2(H^3)}{\partial X^2} \quad \text{...(14)}$$

Eq. (13) transforms into

$$\left[\frac{\partial^2}{\partial X^2} + \left(\frac{L}{2\pi}\right)\frac{\partial^2}{\partial Y^2}\right](H^3P^2) + H^3\left[\frac{\partial^2}{\partial X^2} + \left(\frac{L}{2\pi}\right)^2\frac{\partial^2}{\partial Y^2}\right](P^2) -$$
$$- P^2\left[\frac{\partial^2}{\partial X^2} + \left(\frac{L}{2\pi}\right)^2\frac{\partial^2}{\partial Y^2}\right](H^3) = 0 \quad \text{.....(15)}$$

Eq. (15) expressed in finite difference form using a square mesh yields:

$$(H_3^3 + 2H_0^3 + H_1^3) + \left(\frac{L}{2\pi}\right)^2(H_2^3 + 2H_0^3 + H_0^3)P_0^3 =$$
$$= (H_3^3 + H_0^3)P_3^2 + (H_1^3 + H_0^3)P_1^2 +$$
$$+ \left(\frac{L}{2\pi}\right)^2(H_2^3 + H_0^3)P_2^2 + (H_4^3 + H_0^3)P_4^2 \quad \text{...(16)}$$

This equation was applied by dividing the XY area into an effective 10×20 grid and the numerical solution obtained by a cyclic sequential relaxation of the Gauss-Seidel type using up to 40 per cent over-relaxation to increase the rate of convergence (Ref. 4). The assumption of a pressure distribution symmetrical about the load line reduced by half the field over which the relaxation was applied.

Load Cofficient :

The load carried by an element of area Δx by Δy is given by:

$$f = p_{x,y} \cdot \cos\theta \cdot \Delta x \cdot \Delta y.$$

The total load carried by one land of the bearing is given by:

$$F = \int_0^{2\pi R} \int_0^{l} p \,.\, \cos\theta \,.\, dx\, dy \qquad \text{.....(17)}$$

Introducing dimensionless terms

$$F = \int_0^1 \int_0^1 P \,.\, (\Delta p) \,.\, \cos(2\pi Y) \,.\, d(X \,.\, l)\, d(Y \,.\, 2\pi R) \qquad \text{.....(18)}$$

Hence the load coefficient can be defined as:

$$C_f = \frac{F}{\Delta p \,.\, l \,.\, d} = \pi \int_0^1 \int_0^1 P \,.\, \cos(2\pi Y) \,.\, dX\, dY \qquad \text{.....(19)}$$

The integral was evaluated by Simpson's rule and was found to be sufficiently accurate.

Flow Coefficient :

The side leakage flow through an element of the exit annulus $x = 0$ of width Δy and height Δz is given by:

$$q_x = u \,.\, \Delta y \,.\, \Delta z\Big|_{x=0} \qquad \text{.....(20)}$$

The velocity of flow through the annulus in the x direction u can be shown (Ref. 5) to be:

$$u = \frac{1}{2\mu} \cdot \frac{p}{x} \cdot (z^2 - zh)\Big|_{x=0} \qquad \text{.....(21)}$$

whence q_x can be expressed as:

$$q_x = \frac{1}{2\mu} \cdot \frac{p}{x} \cdot \Delta y \int_0^h (z^2 - zh)\, dz$$

$$= \frac{h^3}{12\mu} \cdot \frac{p}{x} \cdot \Delta y \qquad \text{.....(22)}$$

The total flow through the annulus is then given by:

$$Q = \int_0^{2\pi r} q_x\, dy$$

$$= \frac{1}{12\mu} \cdot \int_0^{2\pi r} h^3 \cdot \frac{p}{x}\, dy\Big|_{x=0} \qquad \text{.....(23)}$$

Using dimensionless forms,

$$Q = \frac{1}{12\mu} \int_0^1 H^3 \; t^3 \frac{\partial(\Delta p \,.\, P)}{\partial(Xl)} \cdot d(2\pi r\, Y)\Big|_{X=0}$$

$$= \frac{\Delta p \,.\, \pi \,.\, dc^3}{12\mu l} \int_0^1 H^3 \frac{\partial P}{\partial X}\, dY\Big|_{X=0} \qquad \text{.....(24)}$$

Hence the flow coefficient can be defined as

$$C_q = \frac{Q\mu l}{\Delta p\, dc^3} = \frac{\pi}{12} \int_0^1 H^3 \frac{\partial P}{\partial X}\, dY\Big|_{X=0} \qquad \text{.....(25)}$$

The term $\dfrac{\partial P}{\partial X}$ appearing in Eq. (25) was evaluated by using the five-point formula (Ref. 5) given in Eq. (26), which was chosen for compatibility of accuracy with Simpson's rule for integration.

$$f'_0 = \frac{1}{12h}(-25 f_0 + 48 f_1 - 36 f_2 + 16 f_3 - 3 f_4) + \frac{h}{5} f^v(\xi) \qquad \text{.....(26)}$$

The computation was programmed in FORTRAN compiler language for a CDC 6400 computer. The input data for each problem were the bearing radius, length, clearance and eccentricity, the gas density, and viscosity, and the inlet and outlet pressures.

The program produced the pressure distribution, load and flow coefficients, actual load and flow, and velocity and Reynolds number distributions.

APPENDIX II

With reference to Fig. 8, the displacement δ at a distance x from the exit end of the land is given by

$$\delta = (l - x) \,.\, \tan\phi \qquad \text{.....(27)}$$

The displacement at a circumferential location $\theta°$ from the position of minimum clearance is given by:

$$\delta = (l - x) \,.\, \tan\phi \,.\, \cos\theta \qquad \text{.....(28)}$$

The film thickness for non-tilted, concentric conditions h is given by:

$$h = c + \frac{x}{l} \,.\, t \qquad \text{.....(29)}$$

The film thickness for tilted conditions (h_t) is given by:

$$h_t = h - \delta$$

$$= c + \frac{x}{l} \,.\, t - (l - x) \,.\, \tan\phi \,.\, \cos\theta \qquad \text{.....(30)}$$

Defining an angularity ratio, A, as

$$A = \frac{e_t}{c}$$

where e_t is the eccentricity at the end of the land for the tilted condition (see Fig. 8), then

$$\tan\phi = \frac{A \,.\, c}{l}$$

and Eq. (30) becomes

$$h_t = c + \frac{x}{l} \,.\, t - \frac{(l - x) \,.\, A \,.\, c}{l} \qquad \text{.....(31)}$$

In terms of the dimensionless groups previously used this becomes:

$$H_t = 1 + X \,.\, T - A(1 - X) \,.\, \cos(2\pi Y) \qquad \text{.....(32)}$$

With H defined by Eq. (32) above, Eq. (3) was solved for pressure as shown in Appendix I.

The righting moment M was evaluated by summing the elemental moments $m_{x,y}$, where $m_{x,y} = p_{x,y} \,.\, \cos\theta \,.\, dx \,.\, dy \,.\, (l - x)$.

Then

$$M = \int_0^{2\pi r} \int_0^{l} (l - x) \,.\, p_{x,y} \,.\, \cos\theta \,.\, dx\, dy \qquad \text{.....(33)}$$

Expressing Eq. (33) in dimensionless terms yields:

$$M = \int_0^1 \int_0^1 l(l - X) \,.\, \Delta p \,.\, P \,.\, \cos(\pi Y) \,.\, d(Xl)\, d(2\pi r\, Y)$$

$$= \Delta p \,.\, l^2 \,.\, d\,\pi \int_0^1 \int_0^1 (l - X) \,.\, P \,.\, \cos(\pi Y)\, dX\, dY \qquad \text{.....(34)}$$

Defining a Moment Coefficient C_M as

$$C_M = \frac{M}{\Delta p \,.\, l^2 \,.\, d} \qquad \text{.....(35)}$$

yields:

$$C_M = \pi \int_0^1 \int_0^1 (l - X) P \,.\, \cos(\pi Y)\, dX\, dY \qquad \text{.....(36)}$$

The integral of Eq. (36) was evaluated by the use of Simpson's rule.